ISSN 2278-2540 | DOI: 10.51583/IJLTEMAS | Volume XV, Issue III, March 2026

Photo Physical Behaviour of Naproxen on DNA, RNA, BSA, Dendrimer and Silver Nanoparticles: Spectral and Molecular Docking Studies

Narayanasamy Rajendiran[1*], Ayyadurai Mani[1], Poomalai Senthilraja[2], S. Senthilmurugan[3]

[1] Department of Chemistry, Annamalai University, Annamalai Nagar, Tamilnadu, India

[2] Department of Bioinformatics, Bharathidasan University, Tiruchy, Tamilnadu, India

[3] Department of Zoology, Annamalai University, Annamalai Nagar, Tamilnadu, India

***Corresponding Author**

DOI: https://doi.org/10.51583/IJLTEMAS.2026.150300117

Received: 31 March 2026; 06 April 2026; Published: 23 April 2026

ABSTRACT

Absorption, emission and molecular docking characteristics of the naproxen drug with (DNA, RNA, BSA, Dendrimer) biomolecules and silver nanoparticles were analysed. With the addition of NP, the absorption and emission maxima of the biomolecules completely disappeared, and no significant spectral shift was noticed in the NP drug. When biomolecule concentrations increased, the absorption and emission intensities of the drug were gradually changed. The negative free energy values indicate the spontaneity of the binding between the drugs and biomolecules. van der Waals force and hydrogen bonding play major roles in the sensing of the drugs and biomolecules. Due to Ag nanoparticles interaction with NP/biomolecules, a blue or red shift was noticed in the absorption and emission spectra. Molecular docking results indicated that the biomolecules interacted with the O and H groups of the NP drug. The sensing behaviour of NP with DNA is higher than other biomolecules. NP drug demonstrates promising anticancer activity through interactions with both the 1r51 and 2oh4 EGFR protein targets.

Keywords: DNA, RNA, BSA, Dendrimer, naproxen, Silver nanoparticles, Anticancer activity

INTRODUCTION

DNA, RNA and BSA-proteins interactions play important roles in a variety of biomolecular functions. Gene expression, transcription, replication, recombination, packaging and repairs all are controlled by DNA-protein interactions. Although the physical basis for these recognition processes is not fully understood, x-ray crystallography, NMR spectroscopy and molecular modelling provide us with a wealth of information on DNA recognitions [1-5]. The quantitative assessment of DNA-protein interaction is essential to understanding transcription, the beginning of biological processes including normal cellular function, development and many diseases [6]. RNA plays a major role in diverse functions within the cell. Protein-RNA complexation is essential in many of these biological functions. Transfer RNAs bind to aminoacyl-tRNA synthetases for the translation of the genetic code during protein synthesis [7,8], while ribonucleoproteins bind RNA in post-transcriptional regulation of gene expression [9]. Although the biological significance of protein complexation with RNA has been well recognized, the specific mechanism of protein-RNA interaction is not fully understood [10]. Measurement of sequence-specific DNA, RNA and BSA-protein interactions is a key experimental procedure in molecular biology of gene regulation.

Numerous studies have experimentally examined the interaction of drugs with deoxyribonucleic acid (DNA), ribonucleic acid (RNA), bovine serum albumin (BSA) and PAMAM-OH (dendrimer). Naproxen [(+)-6-methoxy-et-methyl-2-naphthalene acetic acid, Fig.1] is a non-steroidal anti-inflammatory (NSAID) drug which

ISSN 2278-2540 | DOI: 10.51583/IJLTEMAS | Volume XV, Issue III, March 2026

is recommended for the treatment of rheumatoid arthritis, inflammatory rheumatic disorders, degenerative joint disease, and ankylosing spondylitis. Further, it is useful in lowering the development of granuloma tissue in rats after subcutaneous implantation of cotton pellets laced with carrageenan.

The spectral properties of NP with DNA, RNA, BSA, PAMAM-OH (Dendrimer) have been investigated by using UV-visible, fluorescence and molecular docking methods. Further, we synthesis Ag/NP/biomolecules nanomaterials and characterized by UV-visible and fluorescence methods.

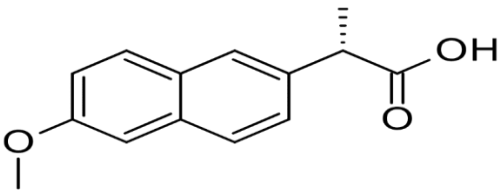

Fig. 1. Chemical structure of Naproxen

Experimental

Preparation of Drug: Biomolecule solution

Solutions comprising biomolecules such DNA, RNA, BSA, or PAMAM-OH dendrimer (1.0×10^{-4} M) were produced in a 10 mL standard volumetric flask at different quantities ranging from 0.1 to 1.0 mL. 0.2 mL of an NP solution (2×10^{-2} M) was added to each flask. After carefully mixing the solutions, triple-distilled water was used to dilute them to a final volume of 10 mL. Each flask's ultimate NP concentration as a result of this process was 4×10^{-4} M.

Preparation of Silver and Ag/NP/Biomolecule Nanoparticles

To prepare silver nanoparticles, 0.01 M silver nitrate was dissolved in 200 mL of deionized water and the solution was heated to 50–60 °C for 30 minutes. While stirring vigorously, 1–2 mL of 1% trisodium citrate solution (prepared by dissolving 1 g of trisodium citrate in 100 mL of deionized water) was added. The formation of silver nanoparticles was confirmed by the appearance of a pale-yellow color [11-14].

To prepare the Ag/NP/biomolecule complex, NP (2×10^{-3} M, dissolved in 20 mL of ethanol) was gradually added to the biomolecule solution (2×10^{-4} M in 80 mL of deionized water). This mixture was heated to 50 °C and stirred continuously on a hot plate with a magnetic stirrer for two hours. Subsequently, 50 mL of the silver nanoparticle solution (0.01 M) was added to 50 mL of the NP/biomolecule solution, and the mixture was stirred for an additional two hours [11-14].

Molecular docking method

AutoDock is a widely utilized software suite for automated molecular docking that employs various techniques such as simulated annealing, local gradient search, and genetic algorithms [15–20]. Version 4.2.6 of AutoDock is freely available under the GNU General Public License (GPL) and can be downloaded from http://autodock.scripps.edu for Linux, macOS, and Windows platforms. Both AutoDock 4.2.6 and AutoDock Vina are commonly used in docking studies. In the present work, docking simulations were carried out using the Lamarckian Genetic Algorithm (LGA) in combination with the Solis & Wets local search method. The initial placement, orientation, and torsional angles of the drug molecules were assigned randomly. Each docking experiment included 10 independent runs, with each run allowing a maximum of 2.5×10^5 energy evaluations. A population size of 150 was maintained. The docking procedure employed a translational step size of 0.2 Å, while the rotational and torsional step sizes were set to 5° [18-20].

Anticancer Potential of naproxen

ISSN 2278-2540 | DOI: 10.51583/IJLTEMAS | Volume XV, Issue III, March 2026

A computational method for examining the intermolecular interactions and binding mechanisms between a pharmacological molecule and a biomolecule is called molecular docking. The micro molecule functions as the ligand in this process, and the macromolecule as the protein receptor. The licensed program Dassault Systèmes BIOVIA Discovery Studio version 22.1.100 was used to perform the docking analysis. Through https://www.rcsb.org/, the target protein's three-dimensional (3D) structure the Epidermal Growth Factor Receptor (EGFR) complexed with epiregulin (EREG) was acquired from the Protein Data Bank (PDB ID: 5WB7). Proteins were prepared by removing ions and water molecules, adding hydrogen atoms, and setting up a grid to find the best binding sites. The interaction between the ligand and the receptor was then examined using docking simulations.

RESULTS AND DISCUSSION

Absorption and emission spectral studies of Naproxen with Biomolecules

Absorption and emission spectral maxima of the naproxen (NP) drug were measured with different concentrations of biomolecules [DNA, RNA, BSA, PAMAM-OH (Dendrimer)] and the relevant data is given in Table 1, Fig. 2. In water, the absorption maxima of NP were appearing at 329, 316, 270, 261, 233 nm and the emission maximum appeared at 352 nm. In the aqueous solution of the isolated DNA, single absorption maximum was appearing at 260 nm while three emission maxima were noticed at 467, 357 and 320 nm. With increasing the DNA concentrations in NP: a) no significant change was observed in the absorption maxima at 329, 316, 282, 230 nm and the absorbance decreased, b) the triple emission maxima of the DNA were lost, while single was emission noticed at 353 nm and the emission intensities decreased.

In the aqueous solution of the isolated RNA, a single absorption maximum was appearing at 258 nm while dual emission was noticed at 362 and 463 nm. With increasing the RNA concentrations with NP: a) no significant shift was noticed in the absorption spectrum at 329, 316, 282 and 230 nm and the absorbance decreased, b) both the shorter and the longer wavelength emissions of the RNA were lost whereas the NP emission noticed at 353 nm, c) the emission intensities decreased at the same wavelength.

Isolated BSA exhibits a single absorption and emission maxima at 278 nm and 336 nm, respectively in the aqueous solution. With increasing the BSA concentration in NP: a) no significant shift was noticed in the absorption spectrum at 329, 316, 270, 262, and 239 nm and the absorbance decreased, b) a single emission was noticed at 353 nm and the emission intensity decreased at the same wavelength.

In aqueous solution the PAMAM-OH which was isolated gives a single absorption maximum appearing at 282 nm, while three emission maxima were noticed at 300, 355 and 440 nm. With increasing the PAMAM-OH concentrations in NP: a) no significant shift was noticed in the absorption spectrum at 329, 316, 270, 262, 235 and the absorbance decreased, b) the triple emission maxima of the PAMAM-OH were lost, while a single emission maximum was noticed at 353 nm, c) the emission intensities decreased at the same wavelength. The absorption and emission results indicate that NP interacted with all the biomolecules. The skeleton structure of the biomolecules restricts the free rotation of the drug molecule; hence, the absorption and emission intensities of the drug were changed in the biomolecule solution.

ISSN 2278-2540 | DOI: 10.51583/IJLTEMAS | Volume XV, Issue III, March 2026

Table 1. Absorption and fluorescence maxima of naproxen [0.2 x 10^{-4} M] with different DNA, RNA, BSA and PAMAM-OH-Dendrimer concentrations [x10^{-6} M].

Concentration of Biomolecules (M)	DNA			RNA			BSA			PAMAM-OH-Dendrimer		
	λ_{abs}	log ε	λ_{flu}	λ_{abs}	log ε	λ_{flu}	λ_{abs}	log ε	λ_{flu}	λ_{abs}	log ε	λ_{flu}
NP only	329	3.25	352	329	3.26	352	329	3.25	352	329	3.25	352
	316	3.24		316	3.23		316	3.24		316	3.24	
	270	3.49		270	3.52		270	3.49		270	3.49	
	261	3.50		262	3.54		261	3.50		261	3.50	
	233	3.79		233	3.83		233	3.79		233	3.79	
0.2	329	3.25	353	329	3.24	353	329	3.16	353	329	3.20	352
	316	3.24		316	3.21		316	3.12		316	3.19	
	270	3.48		275	3.88		270	3.61		270	3.29	
	261	3.47		261	3.62		262	3.62		261	3.28	
	233	3.68					240	3.82		233	3.67	
1.0	329	3.22	353	329	3.17	353	329	3.02	353	329	3.13	353
	316	3.21		316	3.15		316	2.98		316	3.11	
	282	3.21		282	3.13		270	3.46		270	3.23	
	230	3.24		230	3.02		262	3.47		262	3.19	
							239	3.67		235	3.50	
Excitation wavelength (nm)	-	-	270	-	-	270	-	-	270	-	-	270
K (1:1) x10^{5} M^{-1}	-156	-	-121	-125	-	-208	-210	-	-159	-295	-	-213
ΔG (kcalmol^{-1})	-11.34	-	-62.8	-56.6	-	-18.52	-18.7	-	-11.81	-21.3	-	-19.09

ISSN 2278-2540 | DOI: 10.51583/IJLTEMAS | Volume XV, Issue III, March 2026

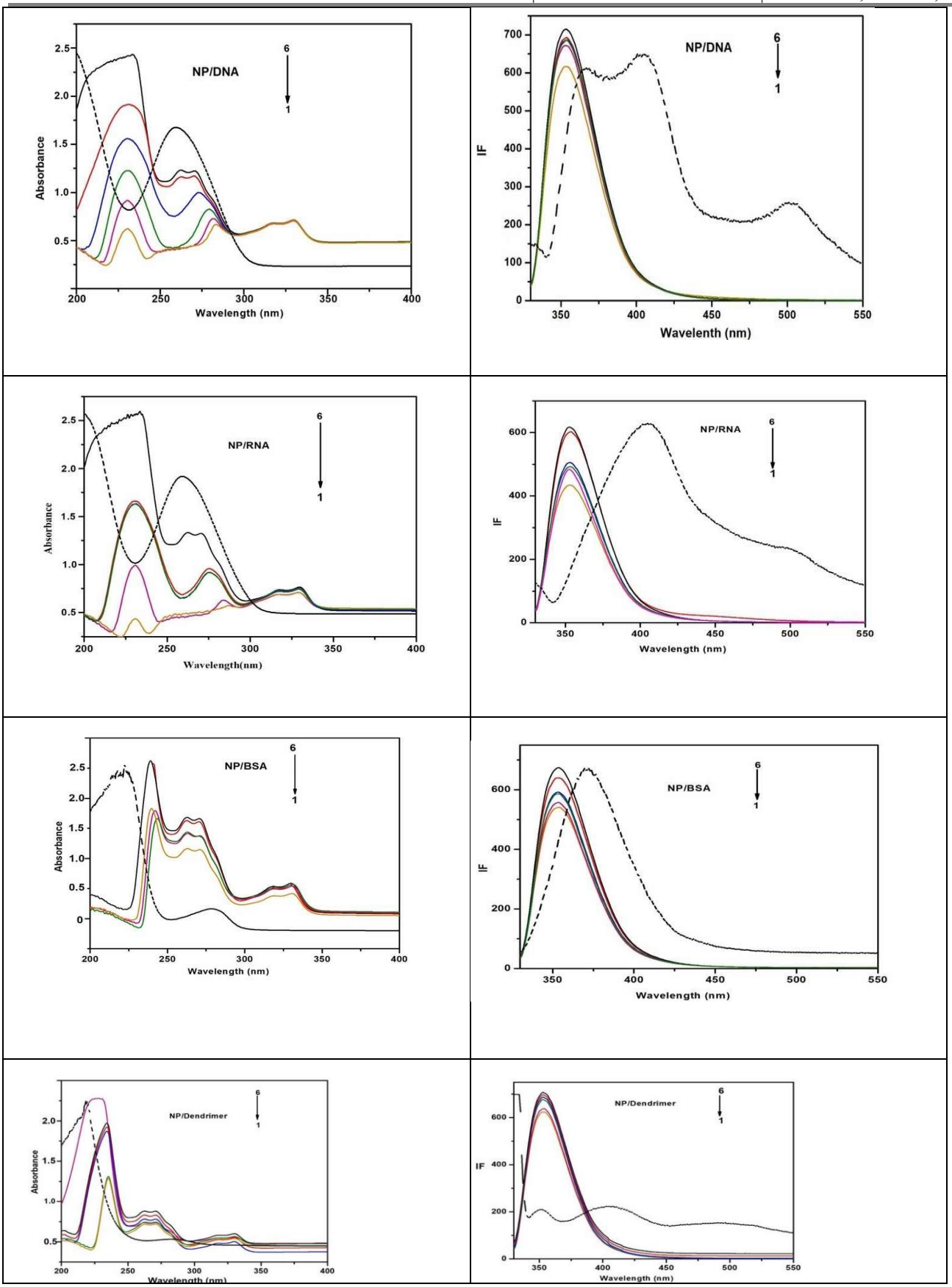

Fig.2. Absorption and fluorescence spectra of naproxen [0.2 x10^{-4} M) with different concentrations of biomolecules (DNA, RNA, BSA, Dendrimer) (M x 10^{-6}): 1) 0, 2) 2, 3) 4, 4) 6, 5) 8, 6) 10, dotted line indicates pure biomolecules spectra.

ISSN 2278-2540 | DOI: 10.51583/IJLTEMAS | Volume XV, Issue III, March 2026

The binding strength of the drugs with biomolecules is mirrored in the intrinsic binding constant K, which represents the binding constant per DNA and RNA base pair and per BSA amino acid. It can be obtained by monitoring the changes in the corresponding absorption wavelength with increasing the concentrations of the biomolecules. From the slope and intercept of the Benesi-Hildebrand plot the binding constant (K) and stoichiometry ratio of the biomolecule interactions were calculated. The presence of an isosbestic point and the plot in the absorption spectrum confirm the formation of a 1:1 complex. Further, the plot of $1/(A-A_0)$ versus $1/[\text{Biomolecules}]^2$ and $1/(I-I_0)$ vs. $1/[\text{Biomolecules}]^2$ gives the concave line suggesting the 1:2 complex is not formed [21-30]. The negative free energy change (ΔG) values (Table 1), reveal that the binding process was spontaneous and thermodynamically stable at the experimental temperature. The negative Δ*G* value indicated the spontaneity of the sensing between drug and biomolecules. ΔG for NP-DNA is more negative than other biomolecules indicated that its sensing behavior is more spontaneous. The change in free energy of NP-DNA is -62.8 kcal mol^{-1}. This also confirms the sensing is higher than that of other drug-biomolecule interactions. In the ground state, the drug sensing behaviour of DNA is higher than other biomolecules, whereas in the excited state, dendrimer is higher than that of other biomolecules.

Drug–biomolecule interactions can be studied by comparison of absorption and emission spectra of the free drug, free DNA, RNA, BSA, PAMAM-OH and drug–biomolecule complexes, which are generally altered. Upon addition of NP drug to the biomolecules, the absorption and emission maxima of the biomolecules are completely disappeared or changed. The absorption and emission maxima of the NP drug are typical results in hyperchromism or hypochromism, hypsochromism (blue shift) and bathochromism (red shift). The gradual change in the absorbance or the emission intensity with the addition of the drug to the biomolecules was attributed to the sensing of the biomolecules. The spectral shifts showed that different functional groups are encapsulated and these functional groups interacted with the biomolecules. The obtained results indicated that it is possible to design the structure of these drug-biomolecule complexes by appropriately selecting the type, length and functional substituent group in the drug.

Because of the intercalative mode involving a stacking interaction between the drug and the base pair of biomolecules, the extent of the blue shift is consistent with the strength of intercalative interaction [31]. The power of this electronic interaction is expected to decrease as the cube of the distance between the drug and the biomolecule base reduces. By decreasing the distance between intercalated drugs and biomolecules, a spectral shift apparently takes place. Thus, this is reliable with the combination of π-π electrons of the drug and the DNA bases. Subsequently, the energy level of the π–π-electron transition decreases, which causes a red or blue shift [32, 33]. In case of electrostatic interaction between the drug and the biomolecule, red or blue shift is observed. This reflects some changes in biomolecule conformation and structure after drug– biomolecule interaction is complete. The red or blue shift is an increase in absorbance of DNA upon denaturation. The two strands of DNA are held together mainly by the stacking interactions, hydrogen bonds and hydrophobic effect between the complementary bases. The hydrogen bond limits the resonance of the aromatic ring so the absorbance of the sample is limited as well. When the DNA double helix is treated with denaturing agents, the interaction force holding the double helical structure is disturbed. The double helix then separates into two single strands which are in the random coiled conformation. At the moment, the base–base interaction gets reduced, increasing the absorption and emission intensities of the biomolecule solution because many bases are in free form and do not form hydrogen bonds with corresponding bases. Red or blue shift reveals the subsequent changes of a biomolecule in its conformation and structure after the drug–biomolecule interaction is completed. Further, the blue shift arises mainly due to the presence of charged cations which bind to biomolecules via electrostatic interaction with the phosphate group of the DNA backbone and thereby causing a reduction and overall damage to the secondary structure of DNA [34]. The blue shift may also be attributed to external contact (electrostatic binding) [35] or to partial uncoiling of the helix structure of DNA, exposing more bases of the DNA [36]. If there is a weaker interaction, then only hypochromic or blue shifts are observed without significant changes of shifts in the spectral profiles [37].

The slight red shift can best be described by the decrease in π-π transition energy of the drugs due to their ordered stacking between the DNA base pairs after intercalation. After binding to the biomolecules, the π-orbital of the binding drug could pair with π- orbital of base pairs in the biomolecules. The coupling π- orbital is generally partially filled by electrons, thus decreasing the transition probabilities, and hence resulting in the

ISSN 2278-2540 | DOI: 10.51583/IJLTEMAS | Volume XV, Issue III, March 2026

blue shift. The compression in the structure of either the drug alone and/or DNA after the formation of drug–biomolecules complex can result in blue shift [38].

As discussed above, the various changes observed in the absorption and emission spectra indicated that the drugs have interacted with DNA, RNA, BSA and PAMAM-OH molecules. This kind of sensing might have caused the slight change in the conformation of drugs. The absorption and emission intensity of these solutions showed moderate shifts towards the wavelength confirmed that the addition of biomolecule is sensing with the drug.

Formation of Ag/NP/Biomolecules Nanoparticle

Absorption and emission spectra of Ag, NP, Ag/NP, Ag/biomolecules, and Ag/NP/biomolecule nanoparticles are analyzed. Ag nanoparticle's absorption and emission bond appear at 420, 250 nm and 474, 352 nm respectively. Further, the yellow color was identified for the formation of Ag nanoparticles [39-45]. An addition of NP solution to the Ag nano, the absorption maxima blue shifted from 420, 250 nm to 332, 318, 268, 260 nm and the emission maxima blue shifted from 474, 352 nm to 354 nm [39-45].

By the addition of DNA solution to the Ag nanoparticles, the absorption maxima red shifted to 436, 262 nm and the emission maxima blue shifted to 470, 423, 362 nm. With the addition of NP/DNA solution to the Ag nanoparticles, no significant changes were noticed in the absorption maxima observed at 329, 316, 261, 230 nm while the emission maxima blue shifted to 440, 353 nm.

While adding RNA to the Ag nano solution, the absorption maxima red shifted to 445, 260 nm and emission maxima shifted to 364, 325 nm respectively. Upon addition of NP/RNA solution to the Ag nanoparticles, no significant changes were noticed in the absorption and emission maxima at 330, 318, 265 nm and 353 nm respectively.

With an addition of BSA to the Ag nano solution, the absorption maxima red shifted to 454, 277 nm and the emission maxima blue shifted to 350 nm respectively. Upon addition of NP/BSA solution to the Ag nanoparticles, no significant changes were noticed in the absorption and emission maxima at 330, 318, 265, 257 nm and 353 nm respectively.

When dendrimer is added to the Ag nano solution, the absorption maxima red shifted to 427, 280 nm and the emission maxima blue shifted to 330, 302 nm respectively. Upon addition of NP/PAMAM-OH solution to the Ag nanoparticles, the absorption maxima red shifted to 450, 337, 262 nm and no significant changes were noticed in the emission maxima at 352 nm. Due to the interaction of Ag nanoparticles with NP, DNA, RNA, BSA and PAMAM-OH dendrimer, red or blue shift was noticed in the absorption and emission spectra. Generally, due to interaction, tends to increase or decrease the intensity of the drug and biomolecules. The spectral variation indicates to confirm the interaction between NP, biomolecules and Ag nanoparticles.

Molecular Docking of NP with biomolecules

The computer-simulated automated docking studies were performed using the widely distributed molecular docking software **Autodock 1.5.6.** In DNA, RNA, BSA and dendrimer, the following protein data bank IDS **1bna**, **2ke6, 3vo3,** and **5d2a** was used. Among the various conformers of docking results, only 10 conformers were taken on the basis of the free energy of binding and score ranking. The minimum binding energy conformer is shown in Figs.3 and 4. The binding energy ΔG_b (kcal/mol), intermolecular energy (kcal/mol), torsional energy, total internal energy, inhibition constant (Ki) (uM), van der Waals + H bond + desolvation energy (kcal/mol), electrostatic energy (kcal/mol), ligand efficiency, unbound energy, refRMS are calculated (Table 2).

In NP drug, the oxygen and hydrogen atoms were docked deeply within the grooves and amino acid of the biomolecules and forming more intercalative sensing or hydrogen bonds with the biomolecules. In DNA, the NP interacted with the nucleotide sites at DG10, DG11, DG12, DG14 and DG16 parts while in RNA, the NP drug interacted with the nucleotide sites at A44, A45, G46, C47, U61. In BSA, the NP drug interacts at ASP814,

ISSN 2278-2540 | DOI: 10.51583/IJLTEMAS | Volume XV, Issue III, March 2026

GLU815, CYS817, GLU818 and ALA881. The NP drug interacts with dendrimer at ASN70. The binding energy, intermolecular energy, total internal energy, van der Waals + H bond + desolvation energy, ligand efficiency of NP with DNA are higher than those of RNA, BSA and dendrimer. The above results suggest that sensing of NP with DNA is higher than with other biomolecules. The higher affinity is presumably attributed to the formation of more and/or tighter hydrogen bonds between the several base pairs at the binding site owing to the increased electronegativity of the hydrogen and oxygen. In other words, they possess the highest potential binding affinity into the binding site of the 3D macromolecule.

Table 2. Naproxen with DNA, RNA, BSA and PAMAM-OH-Dendrimer interaction values.

Various Interactions	DNA	RNA	BSA	Dendrimer
Binding energy ΔGb (kcal/ mol)	7.14	4.38	5.47	5.49
Intermolec. Energy kcal/mol	8.33	5.57	6.66	6.69
Torsional energy	1.19	1.19	1.19	1.19
Total Internal energy	0.27	0.28	0.23	0.27
Inhibition constant (Ki) (uM)	5.85	618.88	97.96	94.1
vdW + H bond + desolv Energy kcal/mol	6.61	5.46	4.68	5.15
Electro static Energy kcal/mol	1.73	0.11	1.98	1.54
Ligand efficiency	0.42	0.26	0.32	0.32
Unbound energy	0.27	0.28	0.23	0.27
refRMS	26.16	30.39	46.3	66.3

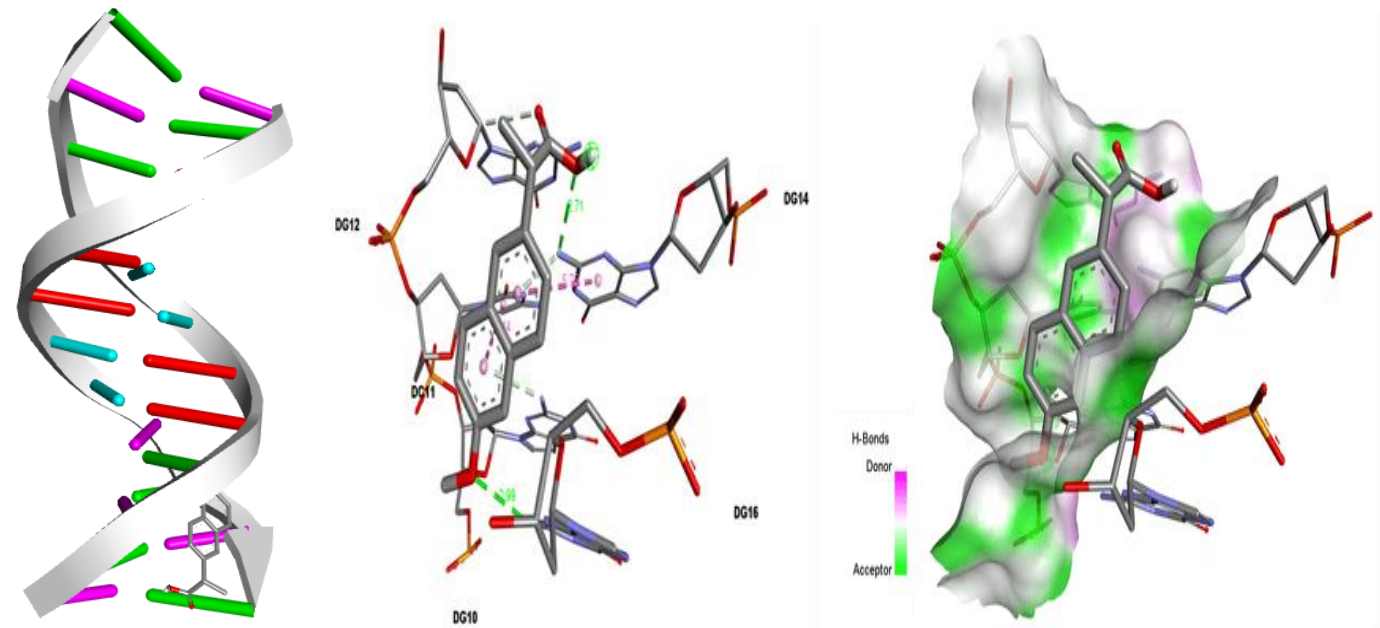

(a) NP/DNA binding image **(b) 3D Interactions** **(c) Hydrogen bond interactions**

ISSN 2278-2540 | DOI: 10.51583/IJLTEMAS | Volume XV, Issue III, March 2026

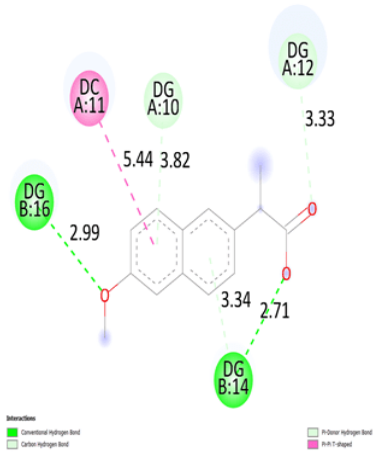

(d) 2D Interactions

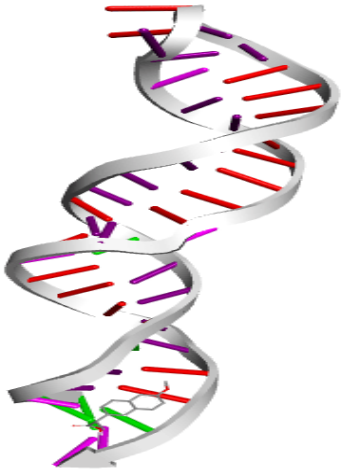

(e) NP/RNA binding image

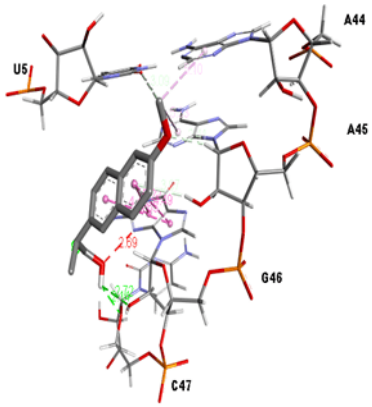

(f) 3D interactions

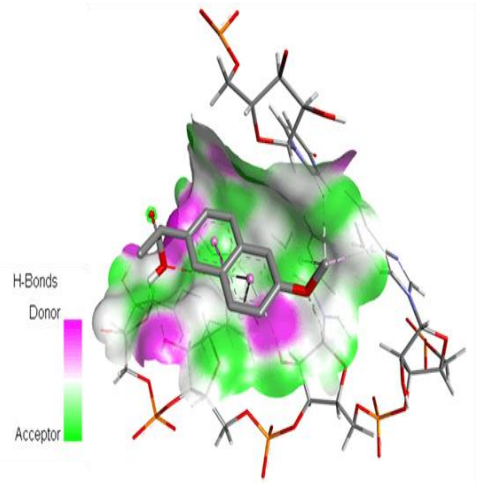

(g) Hydrogen bond interaction

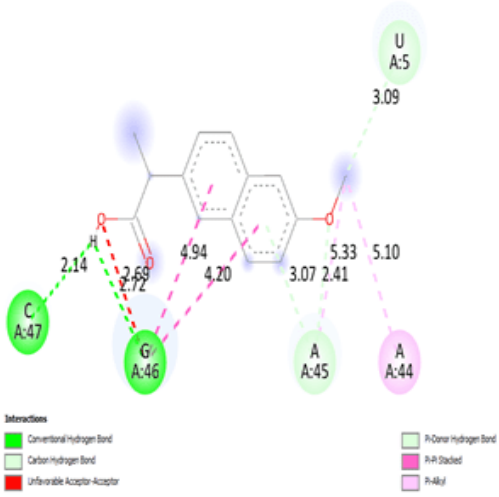

(h) 2D interactions

Fig. 3. Naproxen with biomolecule interaction images for (a-d) NP/DNA binding image, (e-h) NP/RNA binding images.

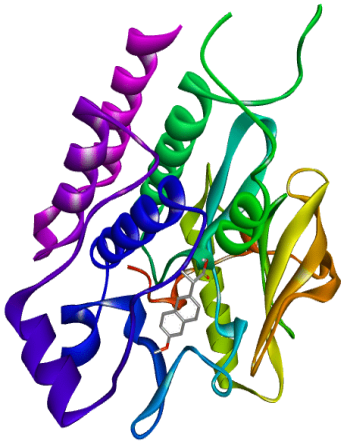

(a) NP/BSA binding image

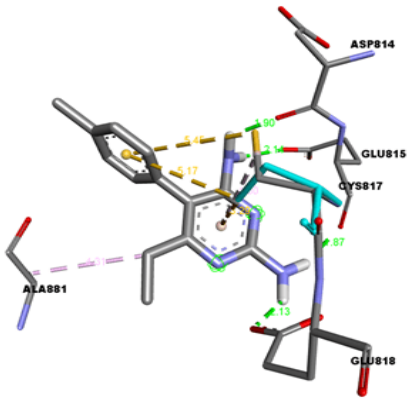

(b) 3D Interactions

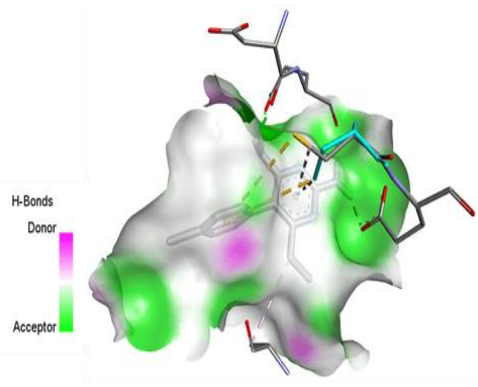

(c) Hydrogen bond interactions

ISSN 2278-2540 | DOI: 10.51583/IJLTEMAS | Volume XV, Issue III, March 2026

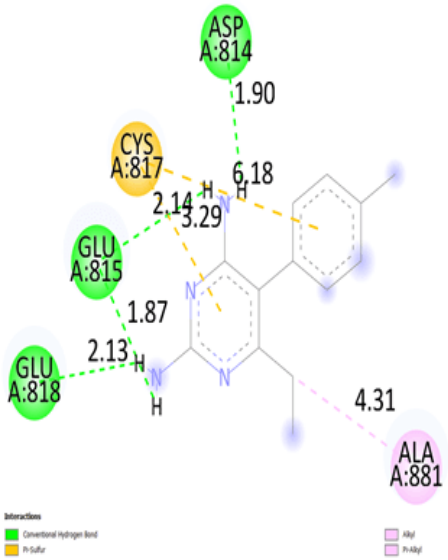

(d) 2D interactions

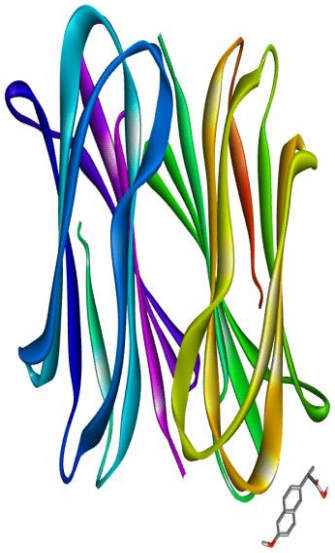

(a) NP/ Dendrimer binding image

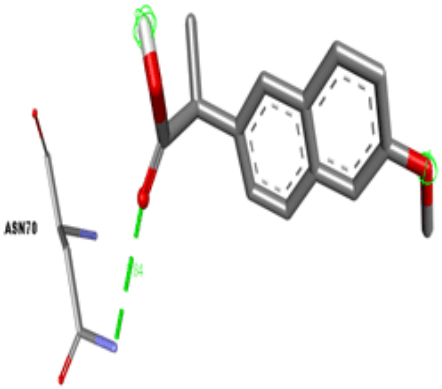

(b) 3D Interactions

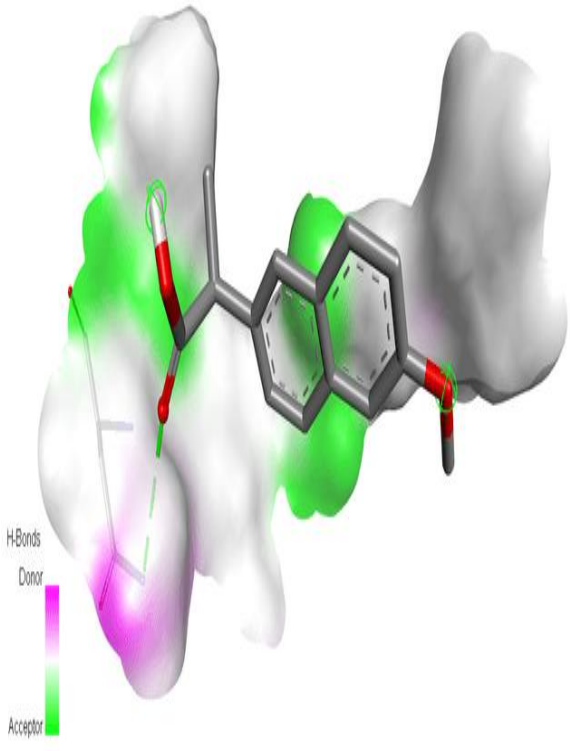

(g) Hydrogen bond interactions

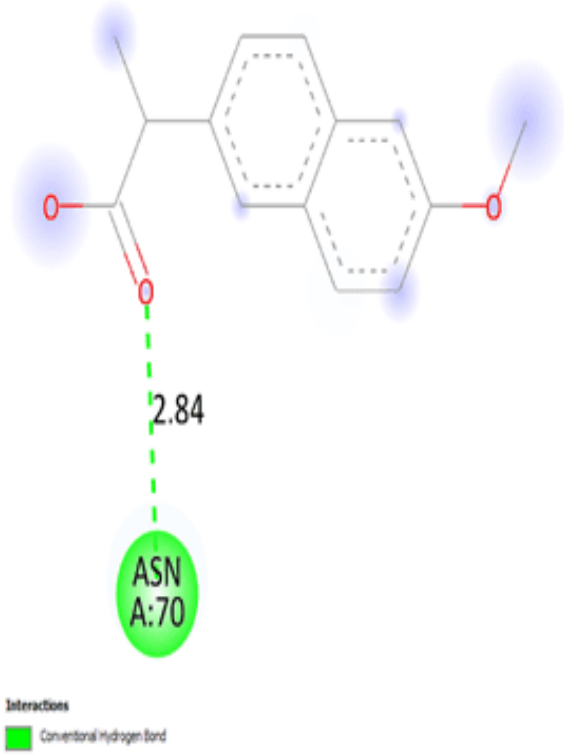

(h) 2D interactions

Fig. 4. Naproxen with biomolecule interaction images for (a-d) NP/BSA binding image, (e-h) NP/Dendrimer binding images.

ISSN 2278-2540 | DOI: 10.51583/IJLTEMAS | Volume XV, Issue III, March 2026

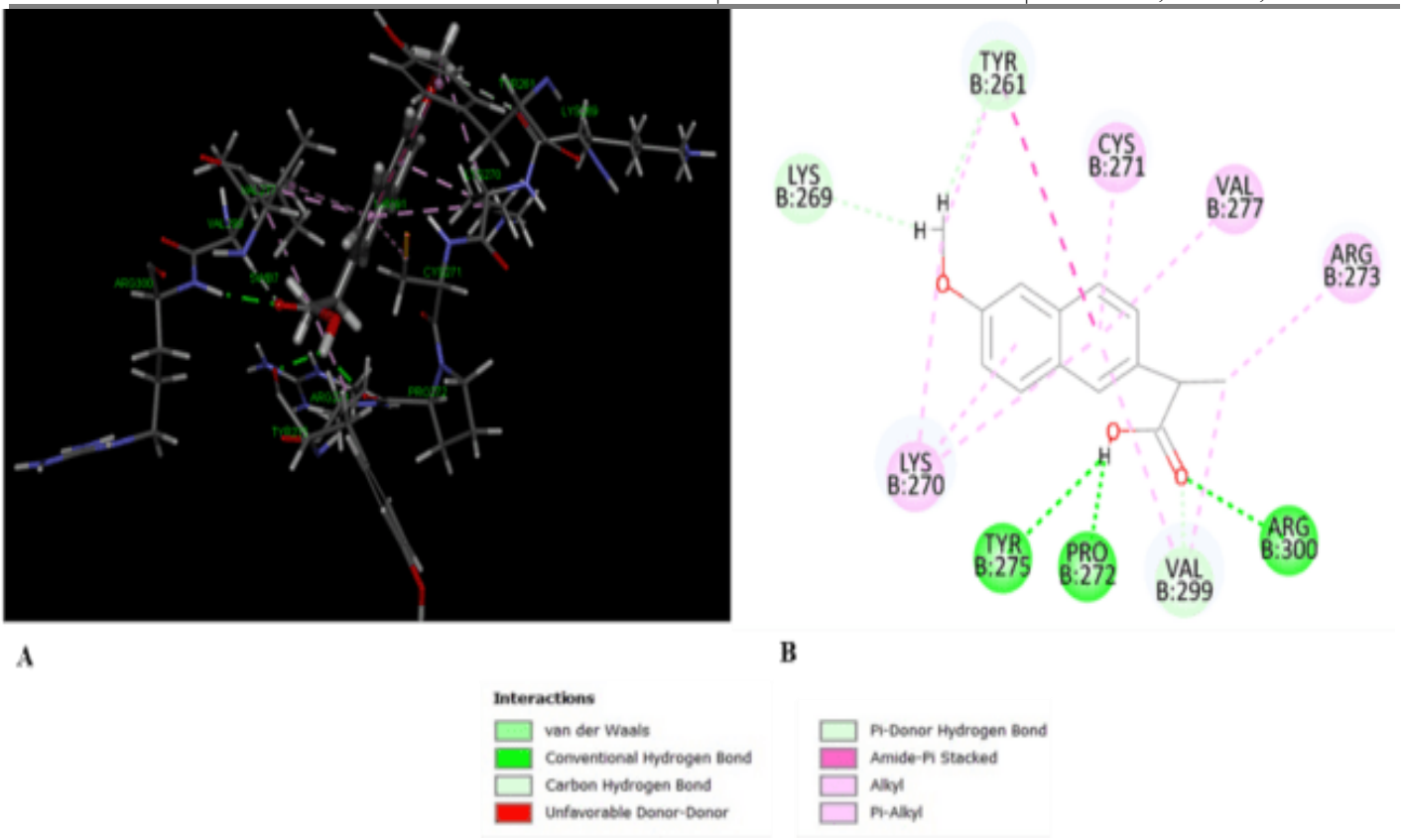

Fig.5. Anticancer potential of naproxen with 1r51 protein

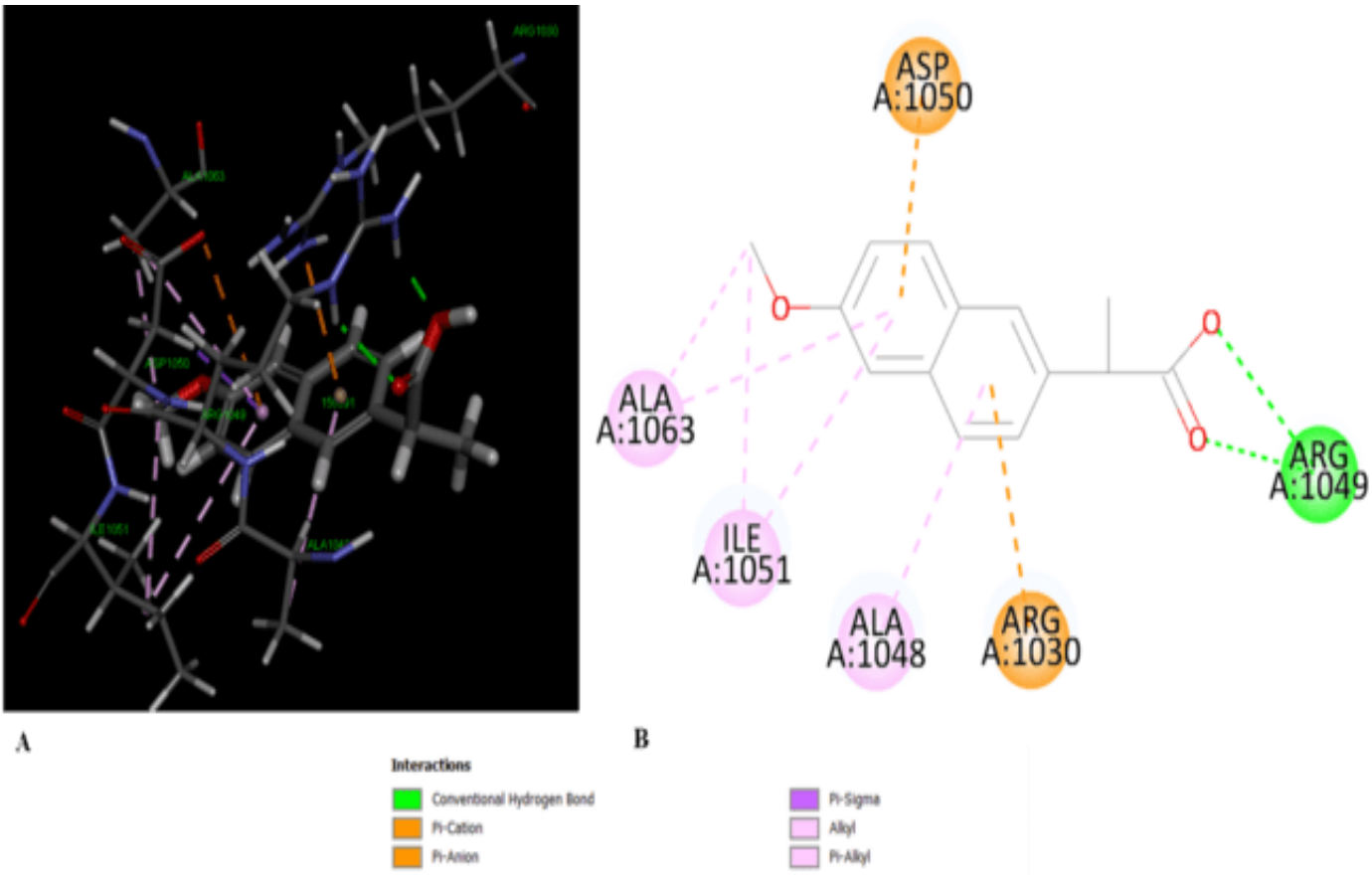

Fig.6. Anticancer potential of naproxen with 2oh4 protein.

ISSN 2278-2540 | DOI: 10.51583/IJLTEMAS | Volume XV, Issue III, March 2026

Anticancer Potential of naproxen

The anticancer potential of NP (ID No. 156391) was assessed through molecular docking studies, as depicted in Figures 5 and 6. In the Figure, 9 and 10 shows the 3D and 2D interactions of the epidermal growth factor receptor (EGFR) complex between epiregulin (EREG) (PDB ID:5WB7) and NP. The specific interactions between NP and the target proteins are summarized below:

With the **1r51 protein**, NP formed three conventional hydrogen bonds at Tyr275, Pro272 and Arg300. Further, four alkyl interactions are observed at Lys270, Cys271, Val277 and Arg273 and two carbon-hydrogen bond interactions are noticed at Lys 269 and Tyr261. The LibDock score is 83.22. With the **2oh4 protein**, NP exhibited a conventional hydrogen bond- Arg1049, Pi-alkyl- Ala1063, Ile1051 & Ala1048. The LibDock score is **95.09**.

Additional evaluation using the AutoDock method yielded the following **ADMET** (Absorption, Distribution, Metabolism, Excretion, and Toxicity) profile for NP: Solubility level is **3;** Blood-Brain Barrier (BBB) penetration is **2;** Extended hepatotoxicity model (EXT Hepatotoxic MD) is **10.4481;** CYP2D6 inhibition prediction is **False;** Hepatotoxicity prediction is **True;** Plasma Protein Binding (PPB) prediction is **True.** *(Note: Drug-induced hepatotoxicity refers to liver damage caused by pharmaceuticals or herbal agents, which is often difficult to diagnose.*

The PPB assessment for siRNA reflects the unbound drug fraction (fu) in plasma under equilibrium conditions. This is a critical parameter in regulatory submissions, as the free drug hypothesis suggests that only the unbound fraction is pharmacologically active at the target site during steady-state conditions. Overall, these results indicate that NP demonstrates promising anticancer activity through interactions with both the 1r51 and 2oh4 EGFR protein targets.

CONCLUSION

Absorption, emission and molecular docking characteristics of the naproxen drug with biomolecules and silver nanoparticles were analysed. With the addition of NP, the absorption and emission maxima of the biomolecules completely disappeared, and no significant spectral shift was noticed in the NP drug. When biomolecule concentrations increased, the absorption and emission intensities of the drug were gradually changed.

The negative ΔG^0 values indicate the spontaneity of the binding between the drugs and biomolecules. The intercalative binding, van der Waals force and hydrogen bonding play major roles in the sensing of the drugs and biomolecules. Due to Ag nanoparticles interaction with NP/biomolecules, blue or red shift was noticed in the absorption and emission spectra.

Molecular docking results indicated that the biomolecules interacted with the O and H groups of the NP drug. The sensing behaviour of NP with DNA is higher than other biomolecules. NP drug demonstrates promising anticancer activity through interactions with both the 1r51 and 2oh4 EGFR protein targets.

REFERENCES

1. Harrison SC. A structural taxonomy of DNA-binding domains. Nature. 1991;353:715–719. https://doi.org/10.1038/353715a0
2. Luisi BF. In: Lilley DMJ (ed) DNA–Protein Interaction at High Resolution. DNA–Protein Structural Interactions. New York: Oxford University Press; 1995. p. 1–48.
3. Luscombe NM, Austin SE, Berman HM, Thornton JM. An overview of the structures of protein–DNA complexes. Genome Biol. 2000;1:1. https://doi.org/10.1186/gb-2000-1-1-reviews001
4. Luscombe NM, Laskowski A, Thornton JM. Amino acid–base interactions: a three-dimensional analysis of protein–DNA interactions at an atomic level. Nucleic Acids Res. 2001;29:2860–2874. https://doi.org/10.1093/nar/29.13.2860

5. Yonezawa M, Doi N, Kawahashi Y, Higashinakagawa T, Yanagawa H. DNA display for in vitro selection of diverse peptide libraries. Nucleic Acids Res. 2003;31:e118. https://doi.org/10.1093/nar/gng119
6. Smolina IV, Demidov VV, Frank-Kamenetskii MD. Pausing of DNA polymerases on duplex DNA templates due to ligand binding in vitro. J Mol Biol. 2003;326:1113–1125. https://doi.org/10.1016/S0022-2836(03)00044-5
7. Namanbhoy T, Morales AJ, Abraham AT, Vortler CS, Giege R, Schimmel P. Simultaneous binding of two proteins to opposite sides of a single transfer RNA. Nat Struct Biol. 2001;8:344–348. https://doi.org/10.1038/87549
8. Moras D. Aminoacyl-tRNA synthetases: structural and functional considerations of the aminoacylation reaction. Curr Opin Struct Biol. 1998;2:138–144.
9. Varani G, Nagai K. RNA recognition by RNP proteins during RNA processing. Annu Rev Biophys Biomol Struct. 1998;27:407–445. https://doi.org/10.1146/annurev.biophys.27.1.407
10. Jones S, Daley DTA, Luscombe NM, Berman HM, Thornton JT. Protein–RNA interactions: a structural analysis. Nucleic Acids Res. 2001;29:943–954. https://doi.org/10.1093/nar/29.4.943
11. Mani A, Ramasamy P, Antony Muthu Prabhu A, Rajendiran N. Investigation of Ag and Ag/Co bimetallic nanoparticles with naproxen–cyclodextrin inclusion complex. J Mol Struct. 2023;1284:135301. https://doi.org/10.1016/j.molstruc.2023.135301
12. Mani A, Venkatesh G, Senthilraja P, Rajendiran N. Synthesis and characterisation of Ag–Co–Venlafaxine–Cyclodextrin nanorods. Eur J Adv Chem Res. 2024;5:9–16. https://doi.org/10.24018/ejchem.2024.5.1.147
13. Mani A, Ramasamy P, Antony Muthu Prabhu A, Senthilraja P, Rajendiran N. Synthesis and analysis of Ag/Olanzapine/Cyclodextrin and Ag/Co/Olanzapine/Cyclodextrin inclusion complex nanorods. Phys Chem Liq. 2024;62:196–209. https://doi.org/10.1080/00319104.2023.2297223
14. Mani A, Ramasamy P, Antony Muthu Prabhu A, Senthilraja P, Rajendiran N. Synthesis and characterisation of Ag/Co/Chloroquine/Cyclodextrin inclusion complex nanomaterials. J Sol-Gel Sci Technol. 2025;115:844–856. https://doi.org/10.1007/s10971-024-06620-5
15. Morris GM, Goodsell DS, Halliday RS, Huey R, Hart WE, Belew RK, Olson AJ. Automated docking using a Lamarckian genetic algorithm and an empirical binding free energy function. J Comput Chem. 1998;19:1639–1662. https://doi.org/10.1002/(SICI)1096-987X(19981115)19:14<1639::AID-JCC10>3.0.CO;2-B
16. Halgren TA. Merck molecular force field. I. Basis, form, scope, parameterization, and performance of MMFF94. J Comput Chem. 1996;17:490–519. https://doi.org/10.1002/(SICI)1096-987X(199604)17:5/6<490::AID-JCC1>3.0.CO;2-P
17. Huey R, Morris GM, Olson AJ, Goodsell DS. A semiempirical free energy force field with charge-based desolvation. J Comput Chem. 2007;28:1145–1152. https://doi.org/10.1002/jcc.20634
18. Morris GM, Lim-Wilby M. Molecular docking. In: Kukol A, editor. Molecular modeling of proteins. Methods Mol Biol. Totowa, NJ: Humana Press; 2008. p. 365–382. https://doi.org/10.1007/978-1-59745-177-2_19
19. Trott O, Olson AJ. AutoDock Vina: improving the speed and accuracy of docking with a new scoring function, efficient optimization, and multithreading. J Comput Chem. 2010;31:455–461. https://doi.org/10.1002/jcc.21334
20. Hill DA, Reilly PJ. Scoring functions for AutoDock. In: Lütteke T, Frank M, editors. Glycoinformatics. Methods Mol Biol. Springer; 2015. p. 467–474. https://doi.org/10.1007/978-1-4939-2343-4_27
21. Rajendiran N, Thulasidhasan J. Interaction of sulfanilamide and sulfamethoxazole with bovine serum albumin and adenine: spectroscopic and molecular docking investigations. Spectrochim Acta A Mol Biomol Spectrosc. 2015;144:183–191. https://doi.org/10.1016/j.saa.2015.01.127
22. Rajendiran N, Thulasidhasan J. Study of the binding of thiazolyazoresorcinol and thiazolyazocresol dyes with BSA and adenine by spectral, electrochemical and molecular docking methods. Can Chem Trans. 2015;3:291–307. https://doi.org/10.13179/canchemtrans.2015.03.03.0209
23. Rajendiran N, Thulasidhasan J. Binding of sulfamerazine and sulfamethazine to bovine serum albumin and nitrogen purine base adenine: a comparative study. Int Lett Chem Phys Astron. 2015;59:170–187. https://doi.org/10.18052/www.scipress.com/ILCPA.59.170

24. Rajendiran N, Thulasidhasan J. Spectral, electrochemical and molecular docking studies on the interaction of dothiepin and doxepin with BSA and DNA base. Luminescence. 2016;31:1438–1447. https://doi.org/10.1002/bio.3126
25. Rajendiran N, Thulasidhasan J. Effects of interaction between non-steroidal anti-inflammatory drugs with BSA and DNA base: spectral, electrochemical and molecular docking methods. J Indian Chem Soc. 2017;94:83–93.
26. Rajendiran N, Thulasidhasan J, Suresh M. Investigation on the interaction of sulfonyl derivatives with BSA and DNA base by spectral and molecular docking analysis. Arch Appl Sci Res. 2017;9:11–18.
27. Rajendiran N, Suresh M. Spectroscopic, electrochemical and molecular docking studies on the biosensing of ofloxacin, norfloxacin with different biomolecules. Int J Chem Pharm Sci. 2017;8:1–18.
28. Rajendiran N, Thulasidhasan J, Suresh M. Interaction of azo dyes with BSA and adenine: spectral, electrochemical and molecular docking methods. Der Pharma Chemica. 2018;10:50–66.
29. Thulasidhasan J, Anandhi R, Venkat Kumar G, Rajendiran N. Interaction of fast garnet GBC with bovine serum albumin: spectral, electrochemical and molecular docking methods. Int J Innov Res Stud. 2018;8:111–119.
30. Rajendiran N, Suresh M. Study of the interaction of ciprofloxacin and sparfloxacin with biomolecules by spectral, electrochemical and molecular docking methods. Int Lett Chem Phys Astron. 2018;78:1–29. https://doi.org/10.18052/www.scipress.com/ILCPA.78.1
31. [31] Liu J, Zhang T, Lu T, Qu L, Zhou H, Zhang Q, Ji L. DNA-binding and cleavage studies of macrocyclic copper(II) complexes. J Inorg Biochem. 2002;91:269–276. https://doi.org/10.1016/S0162-0134(02)00441-5
32. Sirajuddin M, Ali S, Haider A, Shah NA, Shah A, Khan MR. Synthesis, characterization, biological screenings and interaction with calf thymus DNA as well as electrochemical studies of azomethine–organotin(IV) chloride adducts. Polyhedron. 2012;40:19–31. https://doi.org/10.1016/j.poly.2012.03.048
33. Sirajuddin M, Ali S, Shah NA, Khan MR, Tahir MN. Synthesis, characterization, biological screenings and interaction with calf thymus DNA of a novel azomethine derivative. Spectrochim Acta A Mol Biomol Spectrosc. 2012;94:134–142. https://doi.org/10.1016/j.saa.2012.03.068
34. Arjmand F, Jamsheera A. DNA binding studies of new valine-derived chiral complexes of tin(IV) and zirconium(IV). Spectrochim Acta A Mol Biomol Spectrosc. 2011;78:45–51. https://doi.org/10.1016/j.saa.2010.06.009
35. Pratviel G, Bernadou J, Meunier B. DNA and RNA cleavage by metal complexes. Adv Inorg Chem. 1998;45:251–300. https://doi.org/10.1016/S0898-8838(08)60027-6
36. Shahabadi N, Kashanian S, Khosravi M, Mahdavi M. Multispectroscopic DNA interaction studies of a water-soluble nickel(II) complex containing different dinitrogen aromatic ligands. Transit Met Chem. 2010;35:699–705. https://doi.org/10.1007/s11243-010-9382-x
37. Kumar KA, Reddy KL, Vidhisha S, Satyanarayana S. Synthesis, characterization, DNA binding and photocleavage studies of $[Ru(bpy)_2BDPPZ]^{2+}$, $[Ru(dmb)_2BDPPZ]^{2+}$ and $[Ru(phen)_2BDPPZ]^{2+}$ complexes and their antimicrobial activity. Appl Organomet Chem. 2009;23:409–420. https://doi.org/10.1002/aoc.1534
38. Shah A, Zaheer M, Qureshi R, Akhter Z, Nazar MF. Voltammetric and spectroscopic investigations of 4-nitrophenylferrocene interacting with DNA. Spectrochim Acta A Mol Biomol Spectrosc. 2010;75:1082–1087. https://doi.org/10.1016/j.saa.2009.12.061
39. Slistan-Grijalva A, Herrera-Urbina R, Rivas-Silva J, Ávalos-Borja M, Castillón-Barraza F, Posada-Amarillas A. Classical theoretical characterization of the surface plasmon absorption band for silver spherical nanoparticles suspended in water and ethylene glycol. Physica E. 2005;27:104–112. https://doi.org/10.1016/j.physe.2004.10.014
40. Fayaz AM, Balaji K, Girilal M, Kalaichelvan P, Venkatesan R. Myco-based synthesis of silver nanoparticles and their incorporation into sodium alginate films for vegetable and fruit preservation. J Agric Food Chem. 2009;57:6246–6252. https://doi.org/10.1021/jf900337h
41. Sastry M, Mayya K, Bondyopadhyay K. pH-dependent changes in the optical properties of carboxylic acid derivatized silver colloidal particles. Colloids Surf A Physicochem Eng Asp. 1997;127:221–228. https://doi.org/10.1016/S0927-7757(97)00087-3

ISSN 2278-2540 | DOI: 10.51583/IJLTEMAS | Volume XV, Issue III, March 2026

42. Wu S, Yang C, Tsao F, Huang P, Chung M, Li WH. Tunneling magnetoresistance in Ag/Co nanoparticle composites. J Magn Magn Mater. 2005;294:e83–e86. https://doi.org/10.1016/j.jmmm.2005.03.059
43. Wang H, Qiao X, Chen J, Ding S. Preparation of silver nanoparticles by chemical reduction method. Colloids Surf A Physicochem Eng Asp. 2005;256:111–115. https://doi.org/10.1016/j.colsurfa.2004.12.058
44. Garcia-Torres J, Vallés E, Gómez E. Synthesis and characterization of Co@Ag core–shell nanoparticles. J Nanopart Res. 2010;12:2189–2199. https://doi.org/10.1007/s11051-009-9784-x
45. Sobal NS, Hilgendorff M, Moehwald H, Giersig M, Spasova M, Radetic T, Farle M. Synthesis and structure of colloidal bimetallic nanocrystals: the non-alloying system Ag/Co. Nano Lett. 2002;2:621–624. https://doi.org/10.1021/nl025533f